Research paper

Predictive modelling of the impact of silica nanoparticles on fluid loss of water based drilling mud

Richard O. Afolabi*, Oyinkepreye D. Orodu, Ifeanyi Seteyeobot

Department of Petroleum Engineering, Covenant University, P.M.B 1023, Ota, Ogun State, Nigeria

ARTICLE INFO

ABSTRACT

Research into the use of nanoparticles for drilling mud formulation is gaining momentum but a key challenge involves predicting the effect of nanoparticles on the properties of the modified mud. Mathematical models used in the description of drilling muds allow for a generalised computation of drilling performance. In other words, such models cannot quantitatively capture the contributions of nanoparticles to the overall performance of the nano-modified drilling mud. In this work, a new model was derived which describes the fluid loss of nanoparticle enhanced water based drilling mud under static filtration. This was done taking into account the structural kinetics of the bentonite suspension and colloidal behaviour of the nanoparticles. The new fluid loss model was compared with the known API static fluid loss model using statistical measures, Root Mean Square Error (RMSE) and Coefficient of Determination (R^2). The new model compares favourably with the API static model with RMSE and R^2 values of 0.41–0.81 cm^3 and 99.3–99.89% respectively. The new fluid loss model was able to predict a value for the maximum fluid loss. It also accounted for variation in mud cake permeability and solid fraction, which could not be explained by the API fluid loss model.

1. Introduction

Drilling activities for oil and gas is made possible with a drill bit attached to an extended string of drill pipes. The function of the drill bit is to break the rock into cuttings and this is lifted to the surface with the aid of the drilling mud (Sehly et al., 2015; Vryzas and Kelessidis, 2017). At the surface, separation of the cuttings from the drilling mud takes place in an equipment after which the drilling mud is circulated back to the wellbore (Mahmoud et al., 2016; Afolabi et al., 2017a). Additional functions performed by drilling muds include; stabilizing the bare rock surface, regulate subsurface pressures, provide buoyancy, lubricate and cool the drill bit, and prevent contamination of subsurface hydrocarbon fluids (Vryzas and Kelessidis, 2017). As a result, drilling muds must be properly formulated to carry out these functions efficiently in unfavourable downhole environments (Abdo and Danish-Haneef, 2012; Hoelscher et al., 2012; Ismail et al., 2016; Afolabi et al., 2017b; Vryzas and Kelessidis, 2017). Development of new oil and gas fields in difficult subsurface environments entails the formulation and use of sophisticated and unique drilling muds. These drilling muds must be able to preserve their fluid loss and rheological attributes even at harsh downhole conditions (William et al., 2014). In light of this, there has been increased

research into the use of new technologies in advancing oil and gas exploration into these complex terrains and nanotechnology has been at the frontline of new techniques been considered (Vryzas and Kelessidis, 2017). This will open new frontlines in the development of the several hydrocarbon bearing basins (Jain et al., 2015; Taha and Lee, 2015; Ismail et al., 2016). Recent technological advancements made in certain industries such as pharmaceuticals can be attributed to nanotechnology, which has been at the forefront of scientific research and development in the past decade (Afolabi, 2017; Vryzas and Kelessidis, 2017). Nanotechnology covers the engineering of functional systems at the molecular scale. Research into the use of nanotechnology for drilling activities is not an exception to this technological advancement (Vryzas and Kelessidis, 2017). Nanoparticles are essentially made to have dimensions of about 1–100 nm. Colloidal suspensions formed from the dispersion of various nanoparticles in a continuous medium are known to have distinguishing properties for potential applications in various sectors ranging from biomedical to cosmetics, energy and aerospace industries (Vryzas and Kelessidis, 2017). The uniqueness of the physio-chemical properties of these nanoparticles makes them suitable for application in the formulation of drilling mud (Zhang et al., 2012; Jung et al., 2013; Vryzas and Kelessidis, 2017). This is due to their small size alongside the

---

exceptionally high surface-to-volume ratio they possess. This makes nanoparticles most favourable for the formulation of drilling muds, which have appropriate properties to meet demands of challenging downhole conditions (Zakaria et al., 2012; Contreras et al., 2014; Barry et al., 2015). The drilling activities in the oil and gas industry can thus benefit significantly from the use of nanoparticles. Some encouraging prospects in the use of nanoparticles in drilling muds is that it imparts on them excellent characteristics under varied range of environmental conditions (Vryzas and Kelessidis, 2017). In addition, the encouraging prospects in manufacturing specific-type nano-particles will be pivotal towards advancing nanoparticle-based dril-ling muds (Vryzas and Kelessidis, 2017). This is because such modified drilling muds can be formulated to meet the requirements of drilling operations in handling diverse downhole conditions (Ismail et al., 2016; Kang et al., 2016; Vryzas and Kelessidis, 2017). Adoption of new technologies often comes with pronounced risks and this may have been what has limited the use of nanoparticles to laboratory studies with ongoing research for field deployment (Vryzas and Kelessidis, 2017). Modelling the rheological and fluid loss behaviour of nanoparticle-enhanced drilling muds are important when designing and planning for economical drilling operations involving nano-particles (Vryzas and Kelessidis, 2017). Past research efforts have been channelled towards examining the use of different types of nano-particles such as iron oxide nanoparticles, aluminium oxide nano-particles, silicon oxide nanoparticles, polymeric coated nanoparticles and titanium nitride nanoparticles in the preparation of drilling muds. The properties of the modified mud were investigated at different downhole conditions obtainable during drilling operations (Abdo and Danish-Haneef, 2012; Jung et al., 2013; Vegard and Belayneh, 2017; Vryzas and Kelessidis, 2017). The known properties of drilling muds, which can be altered with the use of nanoparticles are wellbore and shale stabilisation, rheology and fluid loss control, wellbore strengthening, cuttings suspension, thermal properties of the drilling muds and magnetic properties (Vryzas and Kelessidis, 2017). Pro-duction of a drilling mud custom-made with nanoparticles to with-stand particular environmental and downhole requirements with ad-justable properties can transform the drilling industry (Fazelabdolabadi and Khodadadi, 2015; Taha and Lee, 2015; Vryzas and Kelessidis, 2017). Promising attempts have been reported with respect to modelling the modified rheological and fluid loss behaviour of nano-drilling muds (Gerogiorgis et al., 2017). This goes to confirm their prospect for describing multifaceted nano-drilling mud systems towards viable application. The known models used in the char-acterisation of bentonite-based muds allow for a generalised descrip-tion of mud behaviour (Gerogiorgis et al., 2017). In such approach for example, rheological models describing shear stress and viscosity are expressed as a data driven correlation or explicit function of shear rate (Gerogiorgis et al., 2017). This does not allow for customisation of such models to explicitly express the aforementioned viscosity and shear stress as a function of multiple independent variables including the contribution of nanoparticles (volume fraction) to the overall model (Gerogiorgis et al., 2017; Vryzas and Kelessidis, 2017). The same applies when describing the fluid loss behaviour of drilling muds treated with nanoparticles. The well-known API static fluid loss model is simply a function of time and parametrised approach is taken when describing the fluid loss of nanoparticle enhanced drilling muds. The contributory effect of nanoparticles in the fluid loss reduction is not captured in the model. In this work, a new model, which describes the fluid loss behaviour of nanoparticle enhanced water based drilling mud formulated from bentonite clay, was derived. This was done taking into account the structural kinetics of the bentonite suspension and colloidal behaviour of the nanoparticles. The developed fluid loss model was compared with the known API static fluid loss model using statistical tools such as the coefficient of determination (R^2) and Root Mean Square Error (RMSE) values.
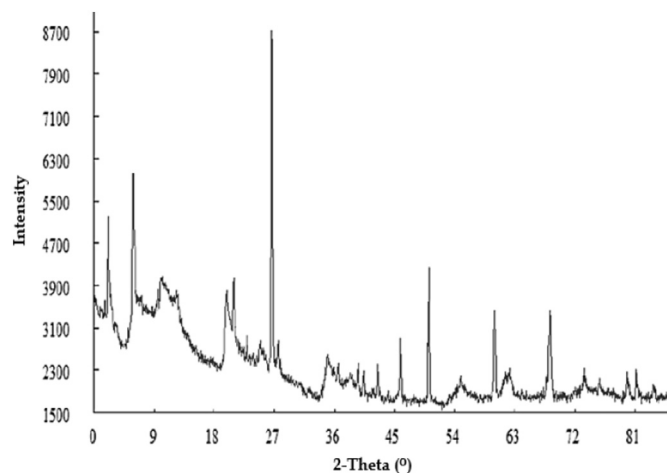

Fig. 1. X-Ray Diffraction (XRD) pattern of bentonite clay.

2. Material and methods

2.1. Materials

2.1.1. Bentonite clay

The local bentonite clay used for this study was sourced from Equilab Solutions in Nigeria. The bentonite clay consist of the mon-tmorillonite mineral. The mineralogical analysis was carried out using the PAN Analytical X-Pert Pro diffractometer operating at 30 kV and 40 mA. The X-Ray Diffraction (XRD) pattern is shown in Fig. 1 with the mineral composition contained in Table 1. Investigation of elemental composition of the bentonite clay was done using Energy Dispersive X-Ray (EDX) spectroscopy. This was carried out using the Phenom® ProX desktop Energy Dispersive X-Ray (EDX) machine. The analysis showed high silica content and the presence of oxides of alkali and alkaline earth metal (Table 2).

2.1.2. Silica nanoparticles

Silica (SiO_2) nanoparticles were also acquired from Equilab Solutions Limited in Nigeria. The nanoparticles were manufactured by Sigma Aldrich and have the following physical properties; appearance: white powder, size: 50 ± 4 nm (TEM), purity: 99.8%, surface area (BET): $60.2 \, m^2/g$.

2.2. Statistical design of experiment

A 2^2 (2-Level, 2-Factors) central composite design was used to create a statistical model to study the quadratic effects and interaction effects between the nanoparticles and bentonite clay particles. MINITAB® 17 (PA, USA) statistical software was used in the design of experiment and statistical analysis of the experimental data. The fluid loss and mud cake thickness (response variables) of the nanoparticle modified water base mud was studied at different concentrations of silica nanoparticles. Nanofluids of varying concentrations were pre-pared by adding 2–10 g of silica nanoparticles in 350 mL of distilled water. The dispersed nanoparticles were stirred using a Hamilton beach mixer at a speed of 11,000 RPM until silica nanofluids were obtained. These nanofluids acts as the base fluids for the preparation of the drilling mud. 20–40 g of the bentonite clay were added to the prepared nanofluid and stirred for 20 min after which the nanoparticle-enhanced water based drilling mud was obtained. The various quantities of na-noparticles and bentonite were selected after preliminary beneficiation experiment. The response variables were fitted by a second-order polynomial in Eq. (1):

Table 1
Mineralogical composition of the bentonite clay.

Mineral	Montmorillonite	Kaolinite	Quartz	Calcite	Feldspar	Biotite
% Composition	22.19	4.91	42.91	12.98	13.78	3.23

Table 2
Compositional analysis of the bentonite clay showing the various oxides present in the clay sample.

Element	SiO_2	Al_2O_3	Fe_2O_3	Na_2O	CaO	K_2O	MgO	TiO_2	LOI
%	55.33	25.69	3.86	4.4	2.65	1.7	2.3	1.1	2.97

$$Y = \beta_o + \beta_{ij}X_iX_j + \sum_{i=1}^{2} \beta_i X_i + \sum_{i=1}^{2} \beta_{ii} X_i^2 \tag{1}$$

Y: the predicted response; β_o: the intercept coefficient; β_i: the linear coefficient; β_{ii}: the squared coefficient; β_{ij}: the interaction coefficient; X_iX_j: the interaction terms; X_i^2: the quadratic terms.

2.3. Fluid loss measurement

The nano-modified water based mud was filtered through the OFITE Low Pressure Low Temperature (LPLT) filter press at 100 psi and 77 °F for low pressure low temperature conditions. For high pressure high temperature fluid loss test, the OFI Testing Equipment (OFITE) High Temperature High Pressure (HTHP) Filter Press was used with pressure range of 300–500 psi and temperatures of 150, 200, 250, 300 °F respectively. The fluid loss was measured for a period of 30 min. The changes in the elemental composition of the formed filter cake arising from the deposition of silica nanoparticles on the cake was analysed using Phenom® ProX desktop Energy Dispersive X-Ray (EDX) Spectroscopy. This approach used in investigating the changes in the elemental composition of the mud cake followed the procedure adopted by Mahmoud et al. (2016).

3. Development of fluid loss model

3.1. Kinetics of mud cake formation during filtration

The state of cohesive bentonite suspensions can be described using the analogy similar to that obtainable in chemical reaction kinetics (Toorman, 1997). This was used to describe the formation of mud cake during filtration process involving drilling muds. A non-dimensional parameter is used in describing the changes in the concentration of clay particles in a bentonite suspension. The value of the non-dimensional parameter is between 0 (low concentration of bentonite suspension) and 1 (high concentration of bentonite suspension). The concentration of clay particles, C, is used as a measure of the amount of clay particles in the bentonite suspension at any given time. The non-dimensional parameter, ζ, is related to the concentration of clay particles at any given time and initial concentration of clay particles, C_o

$$\zeta = \frac{C}{C_o} \tag{2}$$

$$C = C_o \ (\zeta = 1) \tag{3}$$

The rate of diffusion of clay particles to the surface of a mud cake depends on the difference between the maximum concentration of clay particles in the drilling mud, ζ_0 (value of 1) and the concentration of clay particles at any given point in time, ζ. Hence, the rate of diffusion of clay particles is expressed as

$$\frac{d\zeta_r}{dt} = a(\zeta_0 - \zeta)^m \tag{4}$$

where a is the diffusion parameter and m is the diffusion exponent The rate of clay particle build-up on the mud cake is dependent on the time of consolidation of particles on the mud cake, t and concentration of clay particles at any point in time, ζ. The rate of build-up is expressed as

$$\frac{d\zeta_b}{dt} = bt\zeta^{n_b} \tag{5}$$

where b is the build-up constant and n_b is the build-up exponent. The net rate expression is the difference between the rate of diffusion and that of build-up.

$$\frac{d\zeta}{dt} = a(\zeta_0 - \zeta)^m - bt\zeta^{n_b} \tag{6}$$

Assuming a first order rate kinetics for the diffusion and build-up expressions, $m = n_b = 1$.

$$\frac{d\zeta}{dt} = a(\zeta_0 - \zeta) - bt\zeta \tag{7}$$

At equilibrium, the rate of diffusion equals the rate of build-up. Therefore, $\frac{d\zeta}{dt} = 0$

$$a(\zeta_0 - \zeta_e) = bt\zeta_e \tag{8}$$

$$\zeta_e = \frac{a\zeta_0}{a + bt} \tag{9}$$

$$\zeta_e = \frac{1}{1 + \beta t} \tag{10}$$

where β is the ratio of the build-up constant b to the diffusion parameter a.

3.2. Colloidal behaviour of nanoparticles

The theory of colloidal particle behaviour in bentonite suspension follows the description of (Gerogiorgis et al., 2017). The distribution and arrangement of nanoparticles in the suspension was assumed to follow a cubical arrangement with an explicit expression as shown in Eq. (11)

$$h_{np} = 4r_{np} + r_{np}\sqrt[3]{\frac{4\pi}{3\varnothing}} \tag{11}$$

h_{np} is the inter-particle distance between nanoparticles, r_{np} is radius of nanoparticles and $\varnothing$ is fractional volume of nanoparticles. In the absence of shear forces, the inter-particle distance of the nanoparticles in a bentonite suspension is time dependent, inserting Eq. (10), Eq. (11) becomes

$$h_{np} = 4r_{np}\left(\frac{1}{1 + \beta t}\right) + \left(1 - \frac{1}{1 + \beta t}\right)r_{np}\sqrt[3]{\frac{4\pi}{3\varnothing}} \tag{12}$$

3.3. Fluid loss model

The API fluid loss model describing the static filtration process as described by (Darley and Gray, 1988) is given below

$$V_f^2 = \frac{2kPA^2}{\mu}\left(\frac{V_f}{V_c}\right)t \tag{13}$$

P is the pressure differential, k is the permeability of mud cake, μ is the viscosity of the filtrate, V_f is the volume of filtrate, A is area of mud

cake, $\frac{V_f}{V_c}$ is ratio of volume of filtrate to volume of mud cake and t is the time. For a given suspension, $\frac{V_f}{V_c}$ and k in Eq. (13) are constant with respect to time. According to Vipulanandan et al. (2014), the permeability of a mud cake, k and the ratio $\frac{V_f}{V_c}$ are both function of time. In order to account for the time variation of $\frac{V_f}{V_c}$ and k, Eq. (14) is introduced as follows:

$$\frac{V_f}{V_c} = f(\zeta_e, t) \tag{14}$$

The ratio, $\frac{V_f}{V_c}$ is a function of the non-dimensional structural parameter which defines the deposition of solids on the mud cake and time.

$$\frac{V_f}{V_c} = \frac{\alpha}{1 + \beta t}t \tag{15}$$

The volume of mud, V_m, is the sum of the sum of the volume of filtrate, V_f and the volume of mud cake, V_c.

$$V_m = V_f + V_c \tag{16}$$

$$V_f = V_m - V_c \tag{17}$$

$$\frac{V_f}{V_c} = \frac{V_m}{V_c} - 1 \tag{18}$$

The ratio of fraction of solids in the mud cake, f_c to fraction of solids in the mud, f_m is given by Eq. (19)

$$\frac{V_f}{V_c} = \frac{f_c}{f_f} = \frac{f_c}{f_m} - 1 = \frac{\alpha}{1 + \beta t}t \tag{19}$$

The change in permeability of the formed mud cake is a function of the initial permeability of the cake and the non-dimensional structural parameter in Eq. (10).

$$k = f(\zeta_e, k_o) \tag{20}$$

$$\frac{k}{k_o} = \frac{1}{1 + \beta t} \tag{21}$$

k_o is the initial permeability of the formed mud cake. Substituting Eqs. (15) and (21) into Eq. (13), yields

$$V_f = \left[\sqrt[2]{\left(\frac{2P\alpha k_o}{\mu}\right)}\right] A \left[\frac{t}{1 + \beta t}\right] \tag{22}$$

Eq. (12) represents the inter-particle distance between nanoparticles dispersed in a bentonite suspension. Based on the assumption of a cubical arrangement, the cubic volume contribution of nanoparticles to the fluid loss reduction of the suspension is

$$h_{np}{}^3 = \left[4r_{np}\left(\frac{1}{1 + \beta t}\right) + \left(1 - \frac{1}{1 + \beta t}\right)r_{np}\sqrt[3]{\frac{4\pi}{3\emptyset}}\right]^3 \tag{23}$$

The fluid loss model incorporating the contribution of nanoparticles becomes

$$V_f = N\left[\frac{t}{1 + \beta t}\right] + \left[\left(1 - \frac{1}{1 + \beta t}\right)r_{np}\sqrt[3]{\frac{4\pi}{3\emptyset}}\right]^3 \tag{24}$$

The maximum fluid loss becomes

$$\lim_{t \to \infty} V_f = \frac{N}{\beta} + \left[r_{np}\sqrt[3]{\frac{4\pi}{3\emptyset}}\right]^3 \tag{25}$$

The permeability model incorporating the effect of nanoparticles involves comparing Eqs. (12) to (21). This yields Eq. (26)

$$\frac{k}{k_o} = \left[\left(\frac{1}{1 + \beta t}\right) + \left(1 - \frac{1}{1 + \beta t}\right)r_D\sqrt[3]{\frac{4\pi}{3\emptyset}}\right] \tag{26}$$

r_D in Eq. (26) is a dimensionless radius parameter. Eq. (19) was also modified to account for the contribution of nanoparticles by comparing

Table 3
The response surface design and the measured cumulative fluid loss and mud cake thickness.

Run order	Bentonite content (wt%)[a] X	Silica nanoparticles (wt%)[a] Y	Fluid loss (mL)	Cake thickness (cm)
1	6.3	0.0	20.0	0.20
2	6.3	0.5	19.0	0.20
3	6.3	1.0	18.5	0.15
4	6.3	1.5	17.5	0.10
5	13.0	0.0	18.0	0.30
6	13.0	0.5	17.0	0.25
7	13.0	1.0	16.0	0.20
8	13.0	1.5	15.5	0.15
9	15.0	0.0	16.0	0.25
10	15.0	0.5	16.0	0.20
11	15.0	1.0	15.0	0.15
12	15.0	1.5	14.0	0.10

[a] Variables in un-coded levels.

Eqs. (12) to (19). This yields Eq. (27)

$$\frac{f_c}{f_m} - 1 = \left[\left(\frac{\alpha t}{1 + \beta t}\right) + \left(1 - \frac{1}{1 + \beta t}\right)r_D\sqrt[3]{\frac{4\pi}{3\emptyset}}\right] \tag{27}$$

4. Results and discussion

4.1. Statistical analysis of the effect of nanoparticles on drilling mud fluid loss

The influence of bentonite (X) and silica nanoparticles (Y) content on the fluid loss behaviour of the drilling mud was studied using an experimental response surface design. The effect of these factors on the fluid loss behaviour of the nano-modified drilling mud was examined by means of a 2^2 Central Composite Design (CCD). The experimental design and outcome of the investigation carried out is shown in Table 3. Based on the Probability Values (P-Values) which was set at significance level of 5% and the Fischer's Ratio (F-Value), the individual effect of the factors (X, Y) and the interaction between the factors (XY, X^2) play an important role in improving the fluid loss reduction of the formulated drilling mud. The Analysis of Variance (ANOVA) is shown in Table 4. The statistical models relating the various factors to the mud cake thickness (MCT) and cumulative fluid loss (FL) which form the response variables are given below:

$$FL = 18.44 + 0.504X - 1.567Y - 0.0426X^2 \quad R^2 = 0.9860 \tag{28}$$

Table 4
Analysis of Variance (ANOVA) table for regression models (Eqs. (28) and (29)) describing cumulative fluid loss and mud cake thickness.

Source	DF	Adj. SS	Adj. MS	F-value	P-value
ANOVA: cumulative fluid loss (Eq. (28))					
Model	3	34.1	11.4	188.0	0.000
Linear	2	33.7	16.9	278.9	0.000
Square	1	0.79	0.79	13.09	0.007
2-way interaction	–	–	–	–	–
Error	8	0.48	0.06	–	–
Total	11	34.6	–	–	–
ANOVA: mud cake thickness (Eq. (29))					
Model	4	0.04	0.010	88.69	0.000
Linear	2	0.03	0.013	122.7	0.000
Square	1	0.01	0.007	60.50	0.000
2-way interaction	1	0.00071	0.0007	6.36	0.004
Error	7	0.00079	0.0001	–	–
Total	11	0.04063	–	–	–

$$MCT = -0.1837 + 0.0883X - 0.0476Y - 0.003946X^2 + 0.00371XY$$
$$R^2 = 0.9806 \tag{29}$$

The significance and adequacy of the models was tested using ANOVA. The F-value is the extent of deviation in the data about the mean. Here the ANOVA of the regression analysis showed that the quadratic models obtained from the experimental design could sufficiently be applied to forecast the responses as apparent from the high F-values. In addition, the coefficients of correlation (R^2) of the regression equations obtained were 0.9860 for cumulative fluid loss (R^2 adjusted = 0.9808), 0.9806 for the mud cake thickness (R^2 adjusted = 0.9696). These values indicate that the statistical models for the response variables fitted well with the experimental data. The R^2 value for cumulative fluid loss volume indicates that the sample variation of 98.60% is attributed to the factors (bentonite content and silica nanoparticles), and implies that 1.4% of the total variation is not accounted for by the model (Eq. (28)). For the mud cake thickness, the statistical model (Eq. (29)) explains 98.06% of the total variation while the model does not explain 1.94% of the total variation attributed to the factors under consideration. From Eqs. (28) and (29), the response variables (FL and MCT) are significantly affected by the bentonite content (X), and amount of silica nanoparticles (Y). From the regression Eqs. (28) and (29), terms with positive coefficients have to increase for the cumulative fluid loss and mud cake thickness to decrease. The same applies to terms with negative coefficient, which have to decrease for the cumulative fluid loss and mud cake thickness to decrease. The fluid loss of the modified drilling mud decreased compared to the ordinary drilling mud when silica nanoparticles were introduced into the water based drilling mud. The reduction in fluid loss by the silica nanoparticles is due to changes in the elemental composition of the building blocks of the filter cake thereby producing a low permeability medium.

4.2. High pressure high temperature (HPHT) fluid loss test

HPHT fluid loss test was carried out on the drilling muds having silica nanoparticles at a pressure of 300 psi and different temperatures of 150, 200, 250 and 300 °F respectively. This was done to establish the effect of high pressure and temperature. As temperature increased from 150 to 300 °F at constant pressure of 300 psi, the drilling mud treated with silica nanoparticles formed a mud cake with good quality by building a thermally stable clay microstructure. This is evident from the decrease in mud cake permeability (Table 5). The fluid loss result indicates that an increase in the amount of nanoparticles brought about a reduction in fluid lost. This is due to the deposition of nanoparticles bringing about changes in the elemental composition of the building blocks of the mud cake. This resulted in a reduction in the formed mud cake permeability. The obtained fluid loss results from this work tend to confirm the results from the works of Li et al. (2016) and Salih et al. (2016) on drilling mud containing silica nanoparticles. The authors had earlier reported the effect of silica nanoparticles in reducing the fluid loss of drilling mud. Fig. 2 show the impact of the silica nanoparticles on the much-desired need to reduce mud cake permeability while drilling. In order to establish the interfacial phenomenon that exist between the bentonite clay particles and the silica nanoparticles, the composition of the building blocks of the formed filter cake was analysed using EDX. Mud cakes obtained for drilling mud containing 0.5 wt
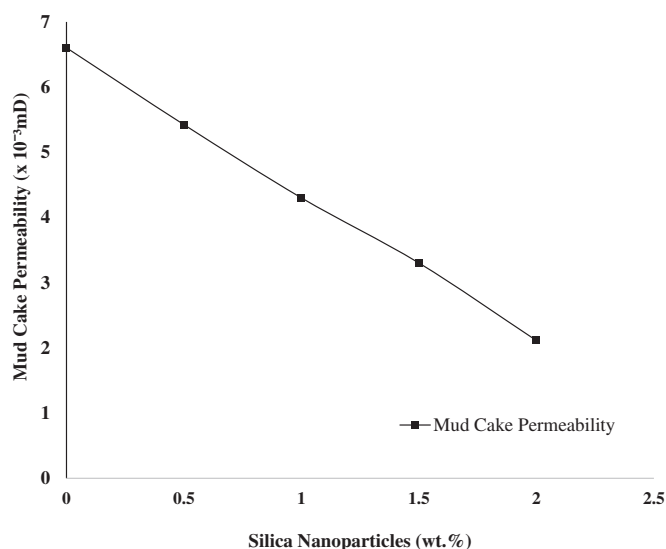

Fig. 2. Effect of silica nanoparticles on the mud cake permeability of 25 g bentonite suspension at 300 psi and 250 °F.

Table 6
Elemental identification analysis of filter cake surface of drilling mud samples at different silica nanoparticle concentration at 300 psi and 250 °F.

Element name	Concentration			
	Base case	0.5 wt%	1.5 wt%	2.0 wt%
Si	15.8	17.1	18.5	19.5
Mg	2.3	1.4	1.1	0.6
Fe	2.7	1.6	1.1	0.6

%, 1.5 wt% and 2.0 wt% silica nanoparticles were analysed for changes in its elemental composition and this was related with a mud sample (base case) having no silica nanoparticles. The EDX analysis (Table 6) showed that an increase in the concentration of the silica nanoparticles resulted in an increase in the silicon (Si^{4+}) wt% and a decrease in the iron (Fe^{2+}) and magnesium (Mg^{2+}) content respectively for the mud cakes obtained at 300 psi and 250 °F. This can be credited to the replacement of the dissociated cations by the silica nanoparticles resulting in a different clay platelet microstructure with reduced permeability (Mahmoud et al., 2016). The high surface area and small size of nanoparticles enables them to form fine dispersions and tight packing structures thereby effectively filling "*fluid flow*" gaps that exist between micron-size particles. This phenomenon also applies to the mud cake, which is formed during the static filtration process involving nano-modified drilling fluids. This reduces the mud cake permeability and subsequently fluid loss. This reduction in fluid loss can also be due to alignment of the clay particles in a face-to-face (FF) configuration, which reduced the surface area available for fluid penetration (Jung et al., 2011). The presence of the silica nanoparticles tend to cause a disruption in the interaction forces between the clay particles necessitating the rearrangement from face-to-edge (FE) to face-to-face (FF) arrangement (Jung et al., 2011). The differential force acting on a drill pipe in contact with a mud cake tend to build up from the time of initial contact up until filtrate leak-off is complete. At this point of complete leak-off, the differential force acting on the drill pipe is at its maximum value. The incidence of differential pipe sticking during oil well drilling can be reduced if the rate of build-up of this differential force can be slowed down. The build-up of the differential force is dependent on the out-flow of filtrate from the formed mud cake which can be controlled by a reduction in cake thickness and permeability. Decreasing the permeability and thickness of the cake using nanoparticles would increase the time required to stick the drill pipe. Thus, the use of silica
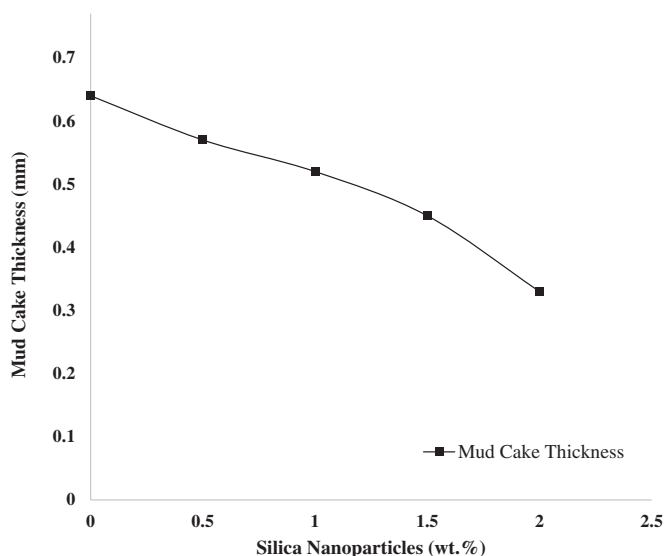
Table 5
Mud cake permeability of drilling mud containing 25 g bentonite and 2.0 wt% silica nanoparticles at 300 psi and different conditions of temperature.

Temperature (°F)	Mud cake permeability ($\times 10^{-3}$ md)
150	3.9524
200	3.8457
250	2.3195
300	2.3039

Fig. 3. Effect of silica nanoparticles on the mud cake thickness of 25 g bentonite suspension at 300 psi and 250 °F.

nanoparticles in a drilling mud leading to a low permeability cake and low cumulative fluid loss is desirable. The area of contact between a drill pipe and the mud cake is dependent on the depth to which the drill pipe sinks in the cake and, as a result, is dependent on the thickness of the mud cake. For this reason also, the mud cake has to be as thin as possible. Figs. 2 and 3 show the incremental effect of the added nanoparticles with respect to the base case without nanoparticles on the mud cake permeability and thickness. Increase in the amount of silica nanoparticles brought about a decrease in the mud cake permeability and thickness.

4.3. Modelling fluid loss behaviour of nano-modified drilling mud

The fluid loss behaviour of the nano-modified drilling mud was modelled using the new model developed for fluid loss prediction. The predicted results of this model was compared with the results obtained also from the API fluid loss model (Eq. (13)) which can also be expressed as

$$V_f = N\sqrt{t} \tag{30}$$

Where, *N* is a constant

$$N = \sqrt{\left[\frac{2kP}{\mu}\left(\frac{V_f}{V_c}\right)\right]} A \tag{31}$$

Based on the API fluid loss model, the mud cake permeability, k and the ratio, $\frac{V_f}{V_c}$ are both assumed constant during the formation of mud cake (Eq. (31)).

4.3.1. Cumulative fluid loss prediction

The cumulative fluid loss prediction was done using the new model in Eq. (24). This was fitted to the experimental fluid loss data obtained and comparison made with the API model. Experimental fluid loss data from four samples containing 4 g (S_1), 6 g (S_2) and 8 g (S_3), of silica nanoparticles dispersed in 25 g bentonite mud were used for the model fitting. The model fitting for sample S_2 showed a coefficient of determination value of 0.994 for the API model while the new fluid loss model was 0.993. Based on the RMSE, the values obtained were 0.417 and 0.558 cm³ for the API and new models respectively. Although the API model seems to be the better fit, the new model was close enough. Samples S_1 and S_3 gave coefficient of determination values of 0.998 and 0.999 for the new model and 0.995 and 0.997 for the API model respectively. The RMSE values were 0.282 and 0.132 cm³ for the new
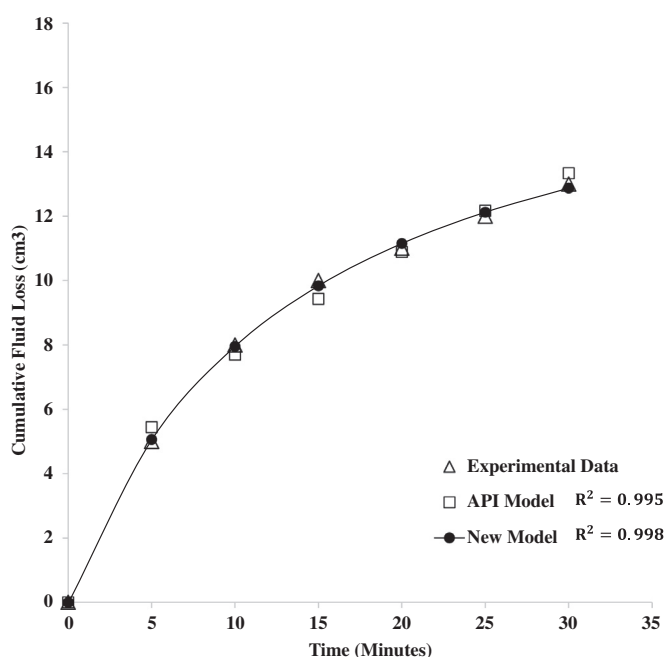

Fig. 4. Cumulative fluid loss prediction using API and new fluid loss model for mud sample S_1 containing 4 g silica nanoparticles and 25 g bentonite at 77 °F and 100 psi.

model and 0.415 and 0.358 cm³ for the API model respectively. The new fluid loss model gave a better prediction for samples S_2 and S_3 based on the statistical measures. Another sample, S_4 containing a lower amount of bentonite, 22.5 g and 6 g of silica nanoparticles was also investigated. The statistical measures for sample S_4 showed coefficient of determination values of 0.992 and 0.989 for the API and new fluid loss models respectively while RMSE values are 0.724 cm³ (API model) and 0.817 cm³ (new model). Plots of the fitted models to the experimental fluid loss data for the various samples are shown in Figs. 4–7. There was an increase in the cumulative fluid loss volume for S_4 when compared with S_2 for the same amount of silica nanoparticles (6 g). This can be explained in terms of a reduction in the volume of solids accompanied with a reduction in the amount of bentonite (22.5 g) in S_4 as compared to S_2 (25 g).
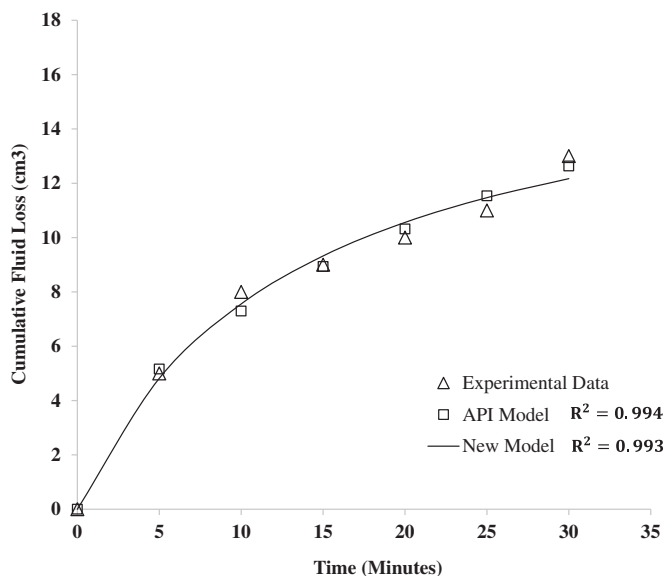

Fig. 5. Cumulative fluid loss prediction using API and new fluid loss model for mud sample S_2 containing 6 g silica nanoparticles and 25 g bentonite at 77 °F and 100 psi.
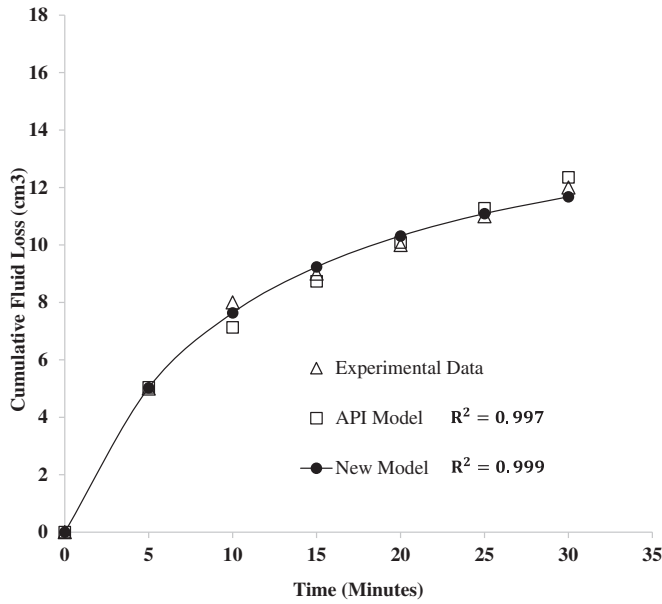
Fig. 6. Cumulative fluid loss prediction using API and new fluid loss model for mud sample S_3 containing 8 g silica nanoparticles and 25 g of bentonite at 77 °F and 100 psi.
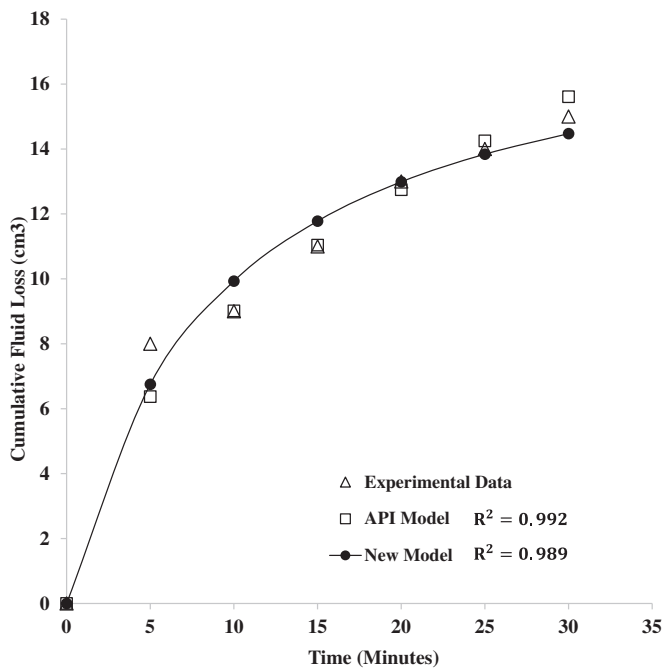

Fig. 7. Cumulative fluid loss prediction using API and new fluid loss model for mud sample S_4 containing 6 g silica nanoparticles and 22.5 g bentonite at 77 °F and 100 psi.

4.3.2. Variation of mud cake permeability

The API fluid loss model predicts a constant value for the mud cake permeability throughout the filtration period. The effect of silica nanoparticles on the mud cake has been established to reduce the permeability thereby reducing the fluid loss volume. The reduction in mud cake permeability by the silica nanoparticles is due to the replacement of dissociated ions in the filter cake thereby producing a lower permeability medium (Mahmoud et al., 2016). Fig. 8 show the comparison between the predicted trend for the cake permeability using the API model and the new model for mud cake permeability (Eq. (26)) for samples S_1, S_2 and S_3. The API model tends to predict a constant value for the mud cake permeability and ratio of solid fraction with time and this only forms the basis for the mechanics of static filtration, which
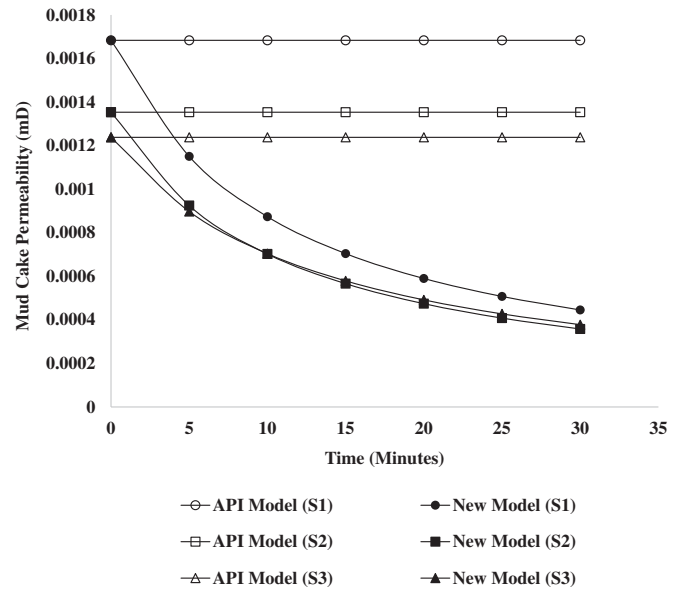

Fig. 8. Mud cake permeability prediction using API and new model for mud samples S_1, S_2, and S_3 containing 4 g, 6 g and 8 g of silica nanoparticles in 25 g bentonite suspension at 77 °F and 100 psi.

constitutes what is presently interpreted for practical purposes (Darley and Gray, 1988). The predicted values for the mud cake permeability using the new model show a decreasing trend with filtration time. The model tends to predict a value for the mud cake permeability at an infinite filtration time from Eq. (26).

At t = ∞,

$$\lim_{t \to \infty} k = \left[r_D\sqrt[3]{\frac{4\pi}{3\varnothing}} \right] k_o \tag{32}$$

At t = ∞, maximum plugging of the pores in the mud cake would have been achieved thereby allowing for no fluid passage. At this point, the mud cake permeability can be taken to be close to zero. The equation in Eq. (32) essentially depicts that permeability reduction of the mud cake in the long run is a function of size and quantity of nanoparticles. Initial permeability reduction during mud cake build up is due to the deposition of the micro-size particles present in the bentonite clay. This is often characterised by a rapid reduction in permeability of the mud cake during the filtration process. Further reduction in the permeability of the mud cake would be due to the presence of nanoparticles. Such reduction in permeability is often a slow process due to the small size of the nanoparticles.

4.3.3. Ratio of solid content in cake and mud

The ratio of solids in the drilling mud to that on the mud cake can be predicted using Eq. (27). The API model has a constant value predicted for the ratio indicating that fraction of solids on the formed mud cake is equal to that in the drilling mud at any given time (Eq. (31)). Fig. 9 show the predicted values of the ratio of volume fraction of solids on the mud cake to that in the drilling mud using the new model for samples S_1, S_2 and S_3. The increase in the values of the ratio is an indication of the deposition of solids as the mud cake is formed with continuous growth with time. At an initial time t = 0, the volume fraction of solids in the mud cake, f_c is zero and f_m is one. This indicates that no mud cake has been formed and the bulk of solids are in the mud. At time t = ∞, Eq. (27) becomes

$$\lim_{t \to \infty} \frac{f_c}{f_m} = 1 + \frac{\alpha}{\beta} + \left(r_D\sqrt[3]{\frac{4\pi}{3\varnothing}} \right) \tag{33}$$

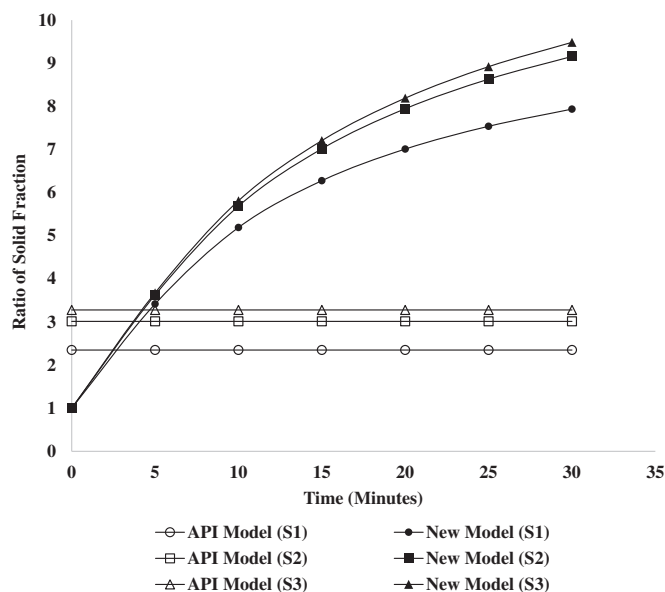Eq. (33) gives the maximum value for the volume fraction of solids,

Fig. 9. Solid fraction prediction using API and new model for mud samples S_1, S_2 and S_3 containing 4 g, 6 g and 8 g silica nanoparticles in 25 g bentonite suspension at 77 °F and 100 psi.

which can be deposited on the formed mud cake. It gives a clear indication of the amount of solids needed to achieve maximum permeability reduction of the mud cake and fluid loss reduction. The values of Eq. (33) obtained for samples S_1, S_2 and S_3 are 11.79, 14.18 and 14.41 respectively. This can be represented as follows

$$f_c = 11.79f_m \quad (34)$$

$$f_c = 14.18f_m \quad (35)$$

$$f_c = 14.41f_m \quad (36)$$

The increased values in the maximum value for the volume fraction of solids from samples S_1, S_2 to S_3 obtained can be attributed to the continuous deposition of solids on the formed mud cake.
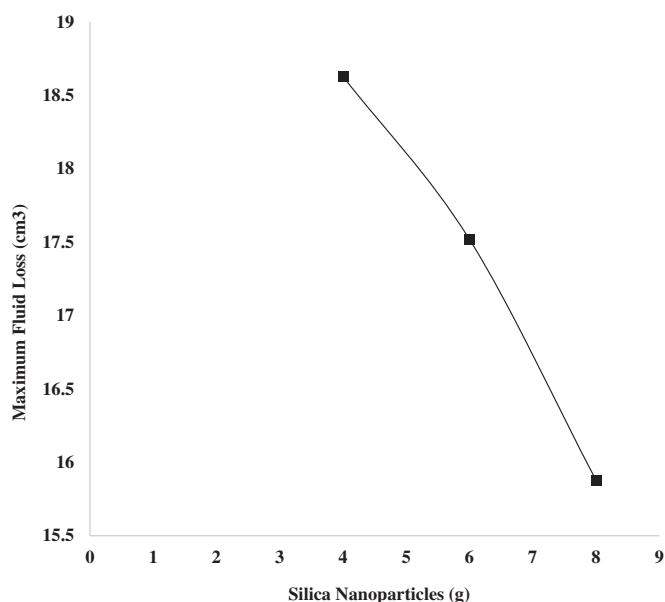

Fig. 10. Effect of silica nanoparticles on the maximum fluid loss as predicted using Eq. (25) at 100 psi and 77 °F. S_1 (4 g), S_2 (6 g) and S_3 (8 g).

4.3.4. Maximum fluid loss prediction

The fluid loss model incorporating the contribution of nanoparticles is as represented in Eq. (24) and the maximum fluid loss in Eq. (25). The maximum fluid loss is representative of the minimum obtainable value of the mud cake permeability. At this point, fluid cannot pass through the formed cake due to plugging of the pore spaces by the solid particles and nanoparticles. The maximum fluid loss predicted by Eq. (25) show a decrease with an increase in the amount of the nanoparticles as represented by samples S_1, S_2 and S_3. The nano-range size of the nanoparticles helps to further reduce the permeability of the formed cake where micro-size particles are not able to plug the pore spaces of the mud cake. Fig. 10 shows the effect of the silica nanoparticles on the maximum fluid loss as predicted from Eq. (25).

5. Conclusion

The impact of silica nanoparticles on the performance of water based muds formulated from bentonite clays was investigated. Furthermore, a new model describing the fluid loss performance of the nanoparticle enhanced drilling mud was also developed. This model was inclusive and able to capture the contribution of nanoparticles to the fluid loss behaviour of the drilling mud. The results obtained from this work yielded the following conclusions:

a) The newly developed model was found to fit the fluid loss profile of the water based mud containing the silica nanoparticles. The new fluid loss model compares favourably with the industry based API static model with R^2 ranging from 0.9989–0.994 and RMSE ranging 0.41–0.81cm^3 respectively.

b) The fluid loss behaviour of the modified drilling mud at a pressure of 300 psi and different temperatures of 150–300 °F resulted in a filter cake with good quality and thermally stable clay microstructure.

c) The reduction in fluid loss can be due to alignment of the clay particles in a face-to-face (FF) configuration, which reduced the surface area available for fluid penetration. The presence of the silica nanoparticles is considered to cause a disruption in the interaction forces between the clay particles necessitating the rearrangement from face-to-edge (FE) to face-to-face (FF) arrangement.

d) The elemental identification analysis showed that an increase in the concentration of the silica nanoparticles resulted in an increase in the silicon (Si^{4+}) wt% and a decrease in the iron (Fe^{2+}) and magnesium (Mg^{2+}) content respectively. This is can be due to the replacement of the dissociated cations by the silica nanoparticles resulting in a different clay platelet microstructure with low permeability.

References

Abdo, J., Danish-Haneef, M., 2012. Nano-enhanced drilling fluids: pioneering approach to overcome uncompromising drilling problems. J. Energy Resour. Technol. 134, 1–6.

Afolabi, R.O., 2017. Modelling the Impact of Silica Nanoparticles on the Performance of Water Based Muds from Nigerian Bentonite Clay (Unpublished). Covenant University, Department of Petroleum Engineering, Ota.

Afolabi, R.O., Orodu, O.D., Efeovbokhan, V.E., 2017b. Properties and application of Nigerian bentonite clay deposits for drilling mud formulation: recent advances and future prospects. Appl. Clay Sci. 143, 39–49.

Afolabi, R.O., Orodu, O.D., Efeovbokhan, V.E., Rotimi, O.J., 2017a. Optimizing the rheological properties of silica nano-modified bentonite mud using overlaid contour plot and estimation of maximum or upper shear stress limit. Cogent Eng. 4, 1–18.

Barry, M.M., Jung, Y., Lee, J.K., Phuoc, T.X., 2015. Fluid filtration and rheological properties of nanoparticle additive and intercalated clay hybrid bentonite drilling fluids. J. Pet. Sci. Eng. 127, 338–346.

Contreras, O., Hareland, G., Husein, M., Nygaard, R., Mortadha, A., 2014. Application of in-house prepared nanoparticles as filtration control additive to reduce formation damage. In: SPE International Symposium and Exhibition on Formation Damage Control. Society of Petroleum Engineers, Lafayette.

Darley, H.C., Gray, G.R., 1988. Composition and Properties of Drilling and Completion Fluids, 5th ed. Gulf Professional Publishing, Houston, TX.

Fazelabdolabadi, B., Khodadadi, A., 2015. Thermal and rheological properties improvement of drilling fluids using functionalized carbon nanotubes. Appl. Nanosci. 5, 651–659.

Gerogiorgis, D.I., Reilly, S., Vryzas, Z., Kelessidis, V.C., 2017. Experimentally validated first-principles multivariate modelling for rheological study and design of complex drilling nanofluid systems. In: SPE/IADC Drilling Conference and Exhibition. Society of Petroleum Engineers, Hague, pp. 1–11.

Hoelscher, K.P., Stefano, G., Riley, M., Young, S., 2012. Application of nanotechnology in drilling fluids. In: SPE International Oilfield Nanotechnology Conference. Society of Petroleum Engineers, Noordwijk, pp. 1–7.

Ismail, A.R., Aftab, A., Ibupoto, Z.H., Zolkifile, N., 2016. The novel approach for the enhancement of rheological properties of water based drilling fluids using multi-walled carbon nanotubes, nanosilica and glass beads. J. Pet. Sci. Eng. 139, 264–275.

Jain, R., Mahto, V., Sharma, V.P., 2015. Evaluation of polyacrylamide-grafted-polyethylene glycol/silica nanocomposite as potential additive in water based drilling mud for reactive shale formation. J. Nat. Gas Sci. Eng. 26, 526–537.

Jung, Y., Barry, M., Lee, J.K., Tran, P., Soong, Y., Martello, D., Chyu, M., 2011. Effect of nanoparticle-additives on the rheological properties of clay-based fluids at high temperature and high pressure. In: AADE National Technical Conference and Exhibition. American Association of Drilling Engineers, Houston, TX.

Jung, C.M., Zhang, R., Chenevert, M., Sharma, M., 2013. High performance water-based mud using nanoparticles for shale reservoirs. In: Unconventional Resources Technology Conference. Society of Petroleum Engineers, Denver, pp. 1–7.

Kang, Y., She, J., Zhang, H., You, L., Song, M., 2016. Strengthening shale wellbore with silica nanoparticles drilling fluid. Petroleum 2, 189–195.

Li, S., Osisanya, S., Haroun, M., 2016. Development of new smart drilling fluids using nano-materials for unconventional reservoirs. In: Abu Dhabi International Petroleum Exhibition & Conference. Society of Petroleum Engineers, Abu Dhabi.

Mahmoud, O., Nasr El-Din, H., Vryzas, Z., Kelessidis, V., 2016. Nanoparticle based drilling fluids for minimizing formation damage in HP/HT applications. In: SPE International Conference and Exhibition on Formation Damage and Control. Society of Petroleum Engineers, Louisiana, pp. 1–26.

Salih, A.H., Elshehabi, T.A., Bilgesu, H.I., 2016. Impact of nanomaterials on the rheological and filtration properties of water based drilling fluids. In: SPE Eastern Regional Meeting. Society of Petroleum Engineers, Canton.

Sehly, K., Chiew, H., Li, H., Song, A., Leong, Y., Huang, W., 2015. Stability and aging behaviour and the formulation of potassium-based drilling muds. Appl. Clay Sci. 104, 309–317.

Taha, N., Lee, S., 2015. Nano-graphene application improving drilling fluds performance. In: International Petroleum Technology Conference. Society of Petroleum Engineers, Doha, pp. 1–16.

Toorman, E.A., 1997. Modelling the thixotropic behaviour of dense cohesive sediment suspensions. Rheol. Acta 36 (1), 56–65.

Vegard, B., Belayneh, M., 2017. The effect of titanium nitride (TiN) nanoparticles on the properties and performance of bentonite drilling mud. Int. J. Nanosci. Nanotechnol. 8 (1), 25–35.

Vipulanandan, C., Raheem, A., Basirat, B., Mohammed, A.S., 2014. New kinetic model to characterize the filter cake formation and fluid loss in HPHT process. In: Offshore Technology Conference. Society of Petroleum Engineers, Houston, TX, pp. 1–17.

Vryzas, Z., Kelessidis, V.C., 2017. Nano-based drilling fluids: a review. Energies 10, 1–34.

William, J.M., Ponmani, S., Samuel, R., Nagarajan, R., Sangwai, J.S., 2014. Effect of CuO and ZnO nanofluids in xanthan gum on the thermal, electrical amd high pressure rheology of water based drilling fluids. J. Pet. Sci. Eng. 117, 15–27.

Zakaria, M.F., Husein, M., Hareland, G., 2012. Novel nanoparticle-based drilling fluid with improved characteristics. In: SPE International Oilfeild Nanotechnology Conference. Society of Petroleum Engineers, Noordwijk, pp. 1–6.

Zhang, Z., Xu, Z., Salinas, B., 2012. High strength nanostructured materials and their oil field applications. In: SPE International Oilfield Nanotechnology Conference. Society of Petroleum Engineers, Noordwijk, pp. 1–6.